RSC Advances

PAPER

View Article Online
View Journal | View Issue

Cite this: *RSC Adv.*, 2025, **15**, 8851

Modulation of fluorescence in novel A–D–A type phenothiazine derivatives *via* oxidation†

Mengdi Lin, *[ab] Shilong Zhang, [c] Xuefeng Liang,[b] Zhenhua Shan,[b] Wenqian Yang[b] and Haijiao Xie[d]

Received 26th February 2025
Accepted 11th March 2025

DOI: 10.1039/d5ra01383f

rsc.li/rsc-advances

1,9-Dimethyl-2,8-funtionalized phenothiazines were successfully developed through a bottom-up synthesis strategy. A high photoluminescence quantum yield of 52% was observed, upon oxidation, and a reduced PLQY of 6% was achieved which opens new avenues for designing PTZ-based push–pull systems with tailored properties.

Organic photoluminescent small molecules have gained great attention in organic photovoltaics,[1–3] organic light-emitting diodes (OLEDs),[4–6] and bioimaging,[7–10] due to their convenience of functionalization and purification. Conventionally, a post-synthesis strategy was widely utilized in the synthesis of photoluminescent small molecules.[11–17] For instance, a copper-catalyzed Ullmann-type C–N coupling reaction was implemented to afford carbazole-substituted thianthrene, exhibiting dual room temperature fluorescence–phosphorescence in air.[17] Despite these significant advancements, achieving high-yield bottom-up synthesis continues to pose a considerable challenge. Consequently, the development of innovative strategies for designing tunable photoluminescent small molecules is imperative.

Phenothiazine (PTZ), a rigid yet dynamically adaptable heterocycle, exhibits a unique ability to fold along its N···S axis. Coupled with its exceptional electron-donating properties, PTZ was extensively utilized as a key component in the design of organic photoluminescent materials.[18–20] To date, the most prevalent strategy for structural modification of the PTZ core has centered on the introduction of substituents at both the nitrogen atom and the 3,7-positions, typically achieved through post-synthetic modification approaches (**A** and **B**).[11–14] For instance, a series of phenothiazine-based push–pull systems with varying sulfur oxidation states were synthesized (**B** and **D**).[21] The higher oxidation states of sulfur substantially enhanced the capabilities of electron injection and transport (**D**). Consequently, modulating the oxidation states of the sulfur atom in the thiazine ring became a widely adopted strategy to alter properties of PTZ derivatives (Fig. 1).[22–24]

However, 2,8-substituted PTZs (2,8-PTZs) were rarely reported due to synthetic difficulties and low yields, limiting their application in photoluminescence (**C**). An effective approach to 2,8-PTZs involved cross-coupling *via* the Buchwald–Hartwig reaction followed by sulfur oxidation.[25] Alternatively, 2,8-PTZs could also be constructed by means of smiles rearrangement of diphenyl sulfide.[26] Therefore, we envisioned that regulation of the oxidation states of sulfur in 2,8-PTZ derivatives could provide deeper insights into PTZ-based push–pull systems.

Herein, we report the facile synthesis of 2,8-functionalized-1,9-dimethyl-phenothiazines, which were further promoted to **JNU-S**, a nonplanar butterfly structure with electron-donating

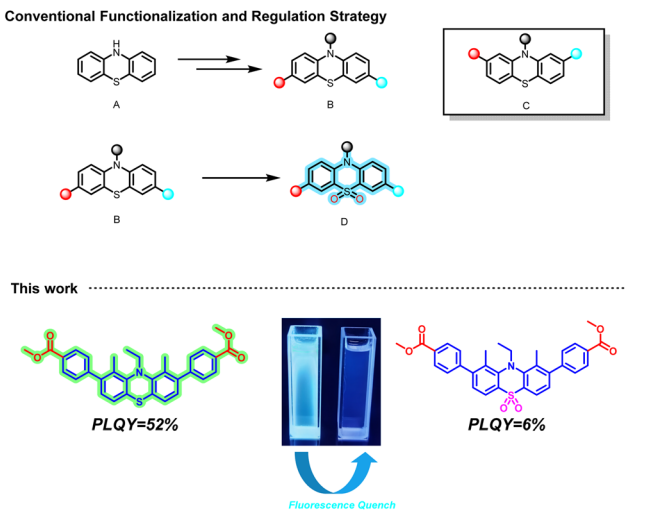

Fig. 1 Conventional functionalization and modulation strategies of PTZ systems (top) and molecular design of **JNU-S** with the modulation of oxidization state.

[a]*College of Pharmacy, Jinan University, Guangzhou, 511400, China. E-mail: linmd6@mail3.sysu.edu.cn*

[b]*Department of CMC, ApicHope Pharmaceutical Group Co., Ltd, Guangzhou, 510760, China*

[c]*National Center for International Research on Green Optoelectronics, South China Normal University, Guangzhou, 510006, China*

[d]*Hangzhou Yanqu Information Technology Co., Ltd, Hangzhou, Zhejiang Province, 310003, China*

† Electronic supplementary information (ESI) available. CCDC 2412799 (for **JNU-S**) and 2412800 (for **JNU-SO$_2$**). For ESI and crystallographic data in CIF or other electronic format see DOI: https://doi.org/10.1039/d5ra01383f

and electron-withdrawing moieties to enhance intramolecular charge transfer (ICT). Upon oxidation to **JNU-SO$_2$**, an unprecedented fluorescence quench emerged, contrasting with the behavior observed in 3,7-functionalized-phenothiazine photoluminescence materials. Furthermore, the structures of both compounds were fully characterized, and their photophysical and optical properties were thoroughly investigated.

The target symmetric A–D–A type PTZ derivatives were synthesized as outlined in Scheme 1. The Buchwald–Hartwig cross-coupling of 1-bromo-3-methoxy-2-methylbenzene **1** and 3-methoxy-2-methylaniline gave compound **2** in 95% yield. **3** was synthesized with sulfur and iodine in 99% yield indicating that regioselectivity issue was effectively resolved by introducing methyl groups at 1,9-positions of PTZ. Finkelstein reaction and S_N2 reaction were simultaneously conducted in one pot to afford **4** in 91% yield. Subsequent demethylation of **4** yielded **5** in 100% yield which was esterified directly with moderate yield of 85% to obtain **6**. The Suzuki–Miyaura cross-coupling between **6** and (4-(methoxycarbonyl)phenyl)boronic acid was subsequently implemented, affording **JNU-S** in 90% yield. **JNU-SO$_2$** was quantitatively isolated through oxidation in the presence of H_2O_2. The structures of these compounds were unambiguously confirmed using high-resolution mass spectroscopy and NMR spectroscopy.

The chemical compositions of **JNU-S** and **JNU-SO$_2$** were elucidated through high-resolution mass spectrometry (HRMS), which revealed prominent signal peaks at *m*/*z* 524.1898 and 556.1798, respectively. These values aligned precisely with the anticipated molecular formulas, as corroborated by the data presented in Fig. S1 and S2.† Furthermore, the structural characterization of these compounds was advanced by ^{1}H NMR spectroscopy, with the spectra of **JNU-S** and **JNU-SO$_2$** depicted in Fig. 2. In the case of **JNU-S**, the aromatic hydrogen atoms manifested as four doublets in an intensity ratio of 2 : 2 : 1 : 1. These signals were meticulously assigned through Nuclear Overhauser Effect (NOE) experiments, as illustrated in Fig. S3.† A notable downfield shift of the aromatic protons in the PTZ moiety was observed, transitioning from 6.98 and 7.17 ppm to 7.28 and 7.97 ppm, a phenomenon attributed to the robust electron-withdrawing conjugation effect. Concurrently, a significant downfield shift was also noted for the methylene protons, which moved from 2.54 ppm to 3.95 ppm, further underscoring the substantial electronic influence exerted by the conjugated system.

The structures of **JNU-S** and **JNU-SO$_2$**, prepared by recrystallization from MeCN were further explicitly confirmed by single crystal X-ray diffraction (SCXRD) analysis (see Fig. 3). Surprisingly, the dihedral angle of **JNU-S** was 146°, significantly smaller than 153° observed in previous studies, suggesting the realization of the regulation of the dihedral angle of PTZ. However, **JNU-SO$_2$** exhibited a dihedral angle of 160°, consistent with PTZ-S,S-dioxide, attributing to the steric effect through sulphone installation and reduced steric hindrance from methyl groups. Additionally, the orthogonal array of the PTZ core (2.915 Å) indicated significant CH–π interactions in **JNU-S**, suggesting a stronger electron-donating effect compared to **JNU-SO$_2$**.

As depicted in Fig. 4, **JNU-S** exhibited a single irreversible oxidation wave at 0.87 V, attributed to the strong electron-donating nature of the phenothiazine unit. In contrast, **JNU-SO$_2$** exhibited a single irreversible oxidation wave at 1.68 V, corresponding to the phenothiazine 5,5-dioxide units. This comparison highlights a notable increase in oxidation potential, reflecting the distinct electronic properties of the two compounds. This rise in oxidation potential aligned with the elevated oxidation state of sulfur and the stabilization of the highest occupied molecular orbital (HOMO) due to the presence of electron-withdrawing groups. The HOMO and LUMO energy levels of **JNU-S** and **JNU-SO$_2$** were determined using the onset potentials of their oxidation and reduction waves, yielding values of −5.11 eV and −5.92 eV, respectively (see Table S3†). These results revealed that the increase in the sulfur oxidation state exerted a more pronounced influence on the HOMO

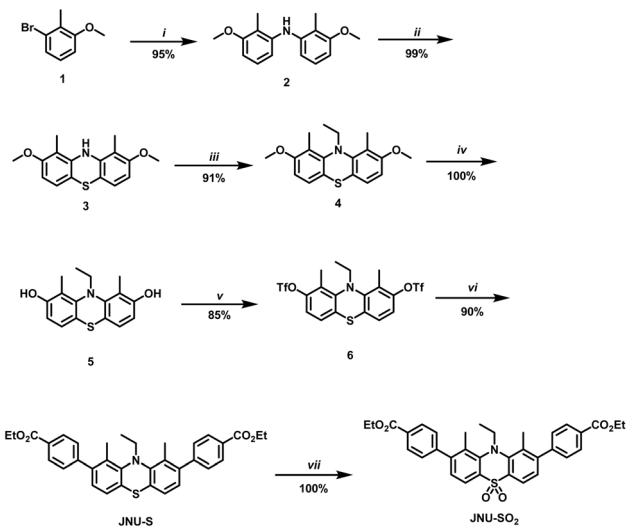

Scheme 1 Synthetic route of **JNU-S** and **JNU-SO$_2$**. Conditions: (i) 3-methoxy-2-methylaniline, $Pd(OAc)_2$, (±)BINAP, Cs_2CO_3, toluene, 90 °C, 12 h; (ii) 1,2-dichlorobenzene, S, I_2, 160 °C, 3 h; (iii) bromoethane, KI, DMSO, NaOH, 70 °C, 5 h; (iv) BBr_3, CH_2Cl_2, 25 °C, 12 h; (v) NaH, $PhNTf_2$, THF, 25 °C, 12 h; (vi) (4-(methoxycarbonyl)phenyl)boronic acid, CsF, $Pd(PPh_3)_4$, 1,4-dioxane, 90 °C, 12 h; (vii) H_2O_2, AcOH, $CHCl_3$, 25 °C, 12 h.

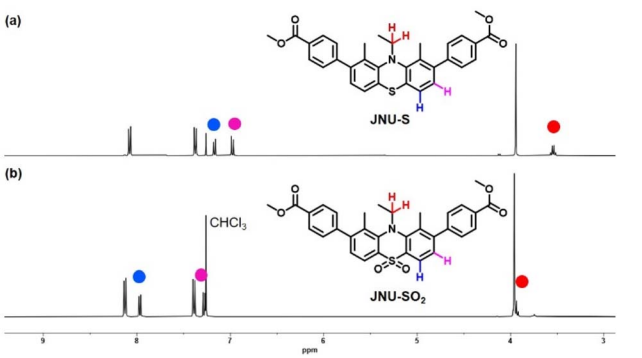

Fig. 2 Partial ^{1}H NMR spectra of **JNU-S** and **JNU-SO$_2$** in $CDCl_3$.

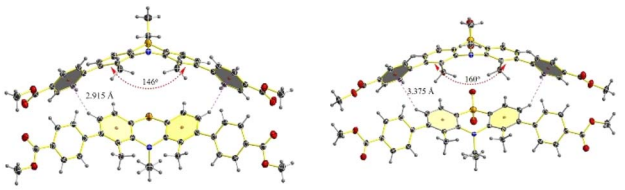

Fig. 3 Single-crystal structures of **JNU-S** (left) and **JNU-SO$_2$** (right).

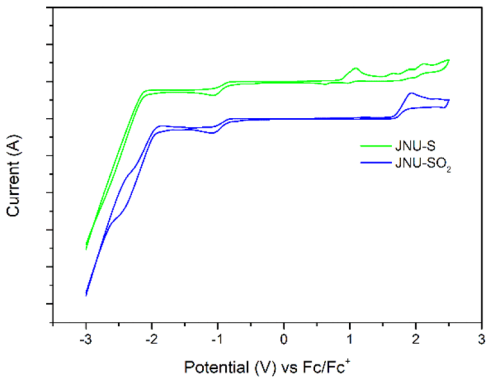

Fig. 4 Cyclic voltammograms of **JNU** (green) and **JNU-SO$_2$** (blue) in 0.1 M solution of Bu_4NPF_6 in dichloromethane at 50 mV s^{-1} scan rate *versus vs.* Ag/AgCl at 25 °C.

energy level compared to the LUMO, underscoring the significant role of sulfur oxidation in modulating the electronic structure of these compounds.

Density functional theory (DFT) calculations were systematically performed to elucidate the electronic and structural characteristics of **JNU-S** and **JNU-SO$_2$**. The inherent butterfly conformation of PTZ conferred a nonplanar structural configuration to both compounds. As illustrated in Fig. 5, the remarkable electron-donating capability of the nitrogen atom localized the highest occupied molecular orbitals (HOMOs) of **JNU** within the heterocyclic ring of PTZ, whereas the benzoyl groups predominantly accommodated the lowest unoccupied molecular orbitals (LUMOs). This electronic distribution engendered a significant stokes shift of 135 nm. In contrast, for **JNU-SO$_2$**, the robust electron-withdrawing nature of the sulfone moiety delocalized the HOMOs across the entire PTZ core. This electronic redistribution resulted in an enlarged HOMO–LUMO energy gap, increasing from 3.93 eV to 4.16 eV, and induced a remarkable blue shift of 105 nm.

As depicted in Fig. 6, the absorption and emission spectra of **JNU-S** and **JNU-SO$_2$** were investigated in chloroform. **JNU-S** showed an absorption band maximized at 370 nm, attributed to ICT, while **JNU-SO$_2$** exhibited a peak at 355 nm. Typically, bathochromic shifts occur due to enhanced ICT effects upon introducing electron-withdrawing groups. However, an unexpected blue shift was observed, likely due to the reduced electron-donating capability of the PTZ core in the A–D–A system. Accordingly, a homologous tendency was emerged when considering the emission maxima system.

The fluorescence quantum yield of **JNU-S** was remarkable (52%) with a lifetime of 2.62 ns in chloroform, comparable to those of PTZ derivatives with high PLQY in A–D–A systems (Table 1 and Fig. S5†). Notably, while oxidation typically increased PLQY, **JNU-SO$_2$** exhibited a dramatic decrease in PLQY (6%), resulting in a fluorescence quench state. This phenomenon, attributed to the stronger electron-withdrawing conjugation in 2,8-PTZ sulfone derivatives, was observed for the first time in A–D–A and A-π-D-π-A PTZ systems, significantly enriching the fluorescence regulation family of PTZ systems. To further clarify unique property uncovered *via* oxidation of **JNU-S**, 3,7-functionalized phenothiazines **JNU-SS** and **JNU-SSO$_2$** were also synthesized, though PLQY decreased from 98% to 37%, fluorescence quench was not observed (Fig. S6, Scheme S1† and Table 1).

To clarify the effect of solvent, the absorption and emission spectra were systematically investigated for **JNU-S** and **JNU-SO$_2$** (Fig. S4†). For **JNU-SO$_2$**, negligible solvent dependence was observed in both absorption and emission spectra, which can be attributed to its small dipole moment and localized excitation (LE) character. In contrast, **JNU-S** displayed a significant bathochromic shift and band broadening in its emission spectrum when transitioning from low-polarity toluene to high-

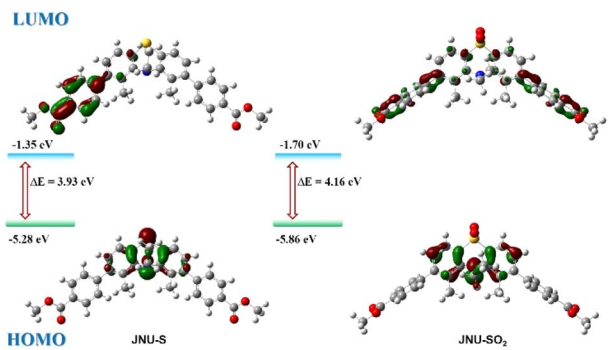

Fig. 5 Optimized structures of **JNU-S** (left) and **JNU-SO$_2$** (right), their HOMO–LUMO and orbital energies were calculated using the B3LYP/6-31G(d,p) basis set.

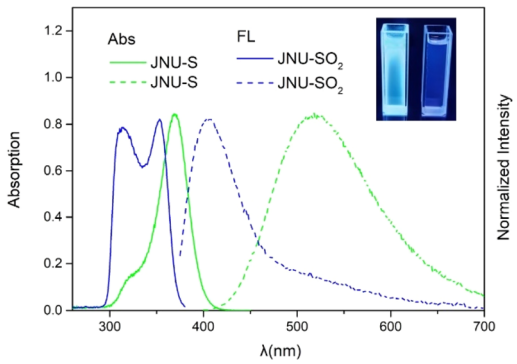

Fig. 6 Normalized absorption (solid) and emission (dash) spectra of **JNU-S** (λ_{ex} = 370 nm) and **JNU-SO$_2$** (λ_{ex} = 355 nm) in $CHCl_3$ ($c = 2.0 \times 10^{-3}$ mol L^{-1}).

Table 1 Partial summary of reported PTZ derivatives consist of A–D–A or A–π–D–π–A system to date

Compound	PLQY	$PLQY_{ox}$ [a]
JNU-S	52%	6%
NPI-PTZ1 (ref. 21)	51%	71%
NPI-PTZ4 (ref. 21)	66%	75%
P1 (ref. 27)	38%	74%
PPP[14]	10%	49%
JNU-SS	98%	37%

[a] S(VI) state of the sulfur atom in the thiazine ring.

polarity acetonitrile, a phenomenon consistent with ICT behavior.

In conclusion, 2,8-functionalized-phenothiazines, **JNU-S** and **JNU-SO_2**, were synthesized through an efficient synthetic strategy. SCXRD analysis revealed that the dihedral angles of **JNU-S** and **JNU-SO_2** were significantly influenced by the oxidation state of sulfur. The oxidation potential of **JNU-SO_2** was notably higher than that of **JNU-S**, reflecting the stabilization of the highest occupied molecular orbital (HOMO) by the electron-withdrawing sulfone moiety. **JNU-S** exhibited a high fluorescence quantum yield (52%) in chloroform, while **JNU-SO_2** displayed an unprecedented fluorescence quench state (6%) due to the strong electron-withdrawing conjugation effect of the sulfone group. This phenomenon contrasted with the typical behavior of 3,7-functionalized PTZ derivatives and enriched the fluorescence regulation mechanisms in PTZ-based systems. DFT calculations confirmed the significant role of sulfur oxidation in modulating the HOMO–LUMO energy gap and electronic distribution. This work demonstrated the potential of 2,8-functionalized PTZ derivatives as versatile materials for optoelectronic applications. Future studies could explore the application of these materials in organic light-emitting diodes (OLEDs), sensors, and other photonic devices.

Data availability

The data supporting this article have been included in the ESI.†

Conflicts of interest

There are no conflicts to declare.

Acknowledgements

We thank ApicHope Pharmaceutical Group Co., Ltd for financial support.

Notes and references

1 A. Mishra and P. Bäuerle, *Angew. Chem., Int. Ed.*, 2012, **51**, 2020–2067.
2 J.-L. Wang, Q.-R. Yin, J.-S. Miao, Z. Wu, Z.-F. Chang, Y. Cao, R.-B. Zhang, J.-Y. Wang, H.-B. Wu and Y. Cao, *Adv. Funct. Mater.*, 2015, **25**, 3514–3523.
3 M. J. Sung, J. Hong, H. Cha, Y. Jiang, C. E. Park, J. R. Durrant, T. K. An, S.-K. Kwon and Y.-H. Kim, *Chem.–Eur. J.*, 2019, **25**, 12316–12324.
4 Q. Wei, N. Fei, A. Islam, T. Lei, L. Hong, R. Peng, X. Fan, L. Chen, P. Gao and Z. Ge, *Adv. Opt. Mater.*, 2018, **6**, 1800512.
5 L. Duan, L. Hou, T.-W. Lee, J. Qiao, D. Zhang, G. Dong, L. Wang and Y. Qiu, *J. Mater. Chem.*, 2010, **20**, 6392–6407.
6 Z. D. Popovic and H. Aziz, *IEEE J. Sel. Top. Quantum Electron.*, 2002, **8**, 362–371.
7 J. Chan, S. C. Dodani and C. J. Chang, *Nat. Chem.*, 2012, **4**, 973–984.
8 H. M. Kim and B. R. Cho, *Chem. Rev.*, 2015, **115**, 5014–5055.
9 T. Terai and T. Nagano, *Pflug. Arch. Eur. J. Physiol.*, 2013, **465**, 347–359.
10 L. Yuan, W. Lin, K. Zheng and S. Zhu, *Acc. Chem. Res.*, 2013, **46**, 1462–1473.
11 J. Liu, X. Zhao, Q. Al-Galiby, X. Huang, J. Zheng, R. Li, C. Huang, Y. Yang, J. Shi, D. Z. Manrique, C. J. Lambert, M. R. Bryce and W. Hong, *Angew. Chem., Int. Ed.*, 2017, **56**, 13061–13065.
12 K. D. Thériault and T. C. Sutherland, *Phys. Chem. Chem. Phys.*, 2014, **16**, 12266–12274.
13 Z. Liu, E. Shi, Y. Wan, N. Li, D. Chen, Q. Xu, H. Li, J. Lu, K. Zhang and L. Wang, *J. Mater. Chem. C*, 2015, **3**, 2033–2039.
14 K. Shanmugasundaram, R. K. Chitumalla, J. Jang and Y. Choe, *New J. Chem.*, 2017, **41**, 9668–9673.
15 A. Tomkeviciene, A. Dabulienė, T. Matulaitis, M. Guzauskas, V. Andruleviciene, J. V. Grazulevicius, Y. Yamanaka, Y. Yano and T. Ono, *Dyes Pigm.*, 2019, **170**, 107605.
16 Y. Wen, H. Liu, S.-T. Zhang, G. Pan, Z. Yang, T. Lu, B. Li, J. Cao and B. Yang, *CCS Chem.*, 2020, **3**, 1940–1948.
17 P. Pander, A. Swist, R. Turczyn, S. Pouget, D. Djurado, A. Lazauskas, R. Pashazadeh, J. V. Grazulevicius, R. Motyka, A. Klimash, P. J. Skabara, P. Data, J. Soloducho and F. B. Dias, *J. Phys. Chem. C*, 2018, **122**, 24958–24966.
18 I. J. Al-Busaidi, A. Haque, N. K. Al Rasbi and M. S. Khan, *Synth. Met.*, 2019, **257**, 116189.
19 F. Khan and R. Misra, *J. Mater. Chem. C*, 2023, **11**, 2786–2825.
20 S. Kumar, M. Singh, J.-H. Jou and S. Ghosh, *J. Mater. Chem. C*, 2016, **4**, 6769–6777.
21 Y. Rout, C. Montanari, E. Pasciucco, R. Misra and B. Carlotti, *J. Am. Chem. Soc.*, 2021, **143**, 9933–9943.
22 Y. Rout, A. Ekbote and R. Misra, *J. Mater. Chem. C*, 2021, **9**, 7508–7531.
23 S. Revoju, A. Matuhina, L. Canil, H. Salonen, A. Hiltunen, A. Abate and P. Vivo, *J. Mater. Chem. C*, 2020, **8**, 15486–15506.
24 I. A. Wright, M. K. Etherington, A. S. Batsanov, A. P. Monkman and M. R. Bryce, *Chem.–Eur. J.*, 2023, **29**, e202300428.
25 W. Luo, Y. Li, L. Wang, Y. Qin, Q. Cheng, G. Hu, C. Yao and X. Song, *Org. Biomol. Chem.*, 2024, **22**, 3725–3731.
26 R. L. Mital and S. K. Jain, *J. Chem. Soc. C*, 1969, 2148–2150, DOI: 10.1039/J39690002148.
27 L. Yao, S. Sun, S. Xue, S. Zhang, X. Wu, H. Zhang, Y. Pan, C. Gu, F. Li and Y. Ma, *J. Phys. Chem. C*, 2013, **117**, 14189–14196.